# A NEW APPROACH TO CONTROL SINGLE-LINK FLEXIBLE ARMS. PART III: Adaptive Control of the Tip Position with Payload Changes

Vicente Feliu[1], Kuldip S. Rattan[2] and H. Benjamin Brown, Jr.

CMU-RI-TR-89-15

The Robotics Institute
Carnegie Mellon University
Pittsburgh, Pennsylvania 15213

July 1989



[1]Visiting Professor, Dpto Ingeniería Eléctrica, Electrónica y Control, UNED, Ciudad Universitaria, Madrid-28040, Spain

[2]Visiting Professor, Department of Electrical Systems Engineering, Wright State University, Dayton, OH. 45435.

# Table of Contents

# List of Figures

# List of Symbols

$\mathcal{A}$ : $n \times n$ constant matrix used in the dynamic model of the beam.

$A(z)$ : discrete compensator for the feedforward term of the motor position control.

$a_i$ : minimum phase zeros of the tip - motor position transfer function.

$\mathcal{B}$ : $n \times 1$ constant matrix used in the dynamic model of the beam.

$B(z)$ : discrete compensator for the feedback term of the motor position control.

$b_i$ : non-minimum phase zeros of the tip - motor position transfer function.

$C_i$ : $1 \times n$ constant matrix used to define the transfer function between mass $m_i$ position and motor position.

$C$ : coupling torque coefficient for the single-mass flexible arm.

$CF$ : Coulomb friction.

$C_t$ : motor - beam coupling torque.

$d(s)$ : denominator of the tip - motor position transfer function.

$E$ : elasticity coefficient of the beam.

$e$ : error between the desired trajectory and the trajectory feasible using a bounded control signal.

$G_c(z)$ : discrete compensator for the tip position.

$g_n(s)$ : transfer function between the tip and motor positions.

$\hat{g}_n(s)$ : transfer function of the optimum feedforward term.

$\mathcal{H}$ : $1 \times n$ constant matrix used in the expression of the motor - beam coupling torque.

$h_i$ $(1 \leq i \leq n)$ : elements of matrix $\mathcal{H}$.

$h_{n+1}$ : coefficient that expresses the influence of the motor angle on the motor - beam coupling torque.

$I$ : cross-section inertia of the beam.

$I_n$ : identity matrix.

$i^*$ : motor current.

$i_c$ : feedforward current term used to compensate for Coulomb friction and motor - beam coupling.

$\mathcal{J}$ : cost index used in optimization problems.

$J$ : inertia of the motor.

$j^*$ : imaginary number.

$K$ : electromechanical constant of the D.C. motor.

$\bar{K}$ : gain of the transfer function between motor and tip position.

$k$ : integer used to represent sampling instants.

$\mathcal{M}$ : $n \times n$ diagonal constant matrix that represents the influence of masses $m_i$ on the dynamics of the beam.

$M(s)$ : transfer function of the motor after decoupling and linearizing by using $i_c$.

$m_i$ $1 \leq i \leq n$ : lumped mass at position $i$.

$m_n'$ : estimated value of the tip mass.

$n$ : number of oscillation modes.

$n_1$ : number of minimum phase zeros.

$n_2$ : number of non-minimum phase zeros.

$P_p$ : reference trajectory, without considering non-minimum phase corrections.

$R_1$ : $2 \cdot n \times 2 \cdot n$ state weighting matrix in the optimization of the tip feedback controller.

$R_2$ : constant that weights the control signal (motor angle) in the optimization of the tip feedback controller.

$s$ : Laplace transform variable.

$T$ : sampling period.

$t$ : time.

$V$ : dynamic friction of the motor.

$x$ : states of the beam.

$\bar{x}$ : x axis of the fixed coordinate system.

$\bar{y}$ : y axis of the fixed coordinate system.

$z$ : z-transform variable.

$\alpha_i$ : coeeficients of the second order factor that appears in the numerator of filter (12).

$\gamma$ : control signal generated by the feedback controller of the tip position.

$\epsilon$ : perturbation in the motor angle.

$\eta$ : input of the decoupled beam system in the minimum phase case.

$\Theta$ : vector of dimension $n$ that represents the angular positions of the lumped masses of the beam.

$\dot{\Theta}$ : vector of dimension $n$ that represents the angular velocities of the lumped masses of the beam.

$\Theta_r$ : position reference of the lumped masses.

$\hat{\Theta}'_r$ : component of the position reference signal that is independent of the tip payload.

$\hat{\Theta}''_r$ : term representative of the component of the position reference signal proportional to the tip payload.

$\theta_i$ $1 \leq i \leq n$ : angular position of mass $m_i$.

$\dot{\theta}_i$ $1 \leq i \leq n$ : angular velocity of mass $m_i$.

$\theta_m$ : motor angular position.

$\theta_{mr}$ : reference of the motor angular position.

$\hat{\theta}_{mr}$ : feedforward signal for the tip control.

$\hat{\theta}'_{mr}$ : component of the feedforward signal that is independent of the tip payload.

$\hat{\theta}''_{mr}$ : coefficient of the component of the feedforward signal proportional to the tip payload.

$\theta_n$ : angular position of the tip.

$\theta_{nr}$ : reference of the angular position of the tip.

$\Lambda$ : $2 \cdot n$ row vector that represents a "P.D. type" feedback controller for the tip position.

$\Lambda_1$ : $n$ row vector that represents the "P." terms of the feedback controller for the tip position.

$\Lambda_2$ : $n$ row vector that represents the "D." terms of the feedback controller for the tip position.

$\lambda_i, \lambda_j$ : elements of vector $\Lambda$.

$\pi$ : $\pi$ number.

$\rho$ : ratio between the estimated tip mass and the nominal tip mass.

$\tau_1, \tau_2$ : variables used to integrate in function of time.

$\Upsilon$ : $n$ column vector of transfer functions that relates the references for the position of masses $m_i$ with the reference for the tip angle.

* variables are also used as integer indexes to represent elements of other vectorial variables.

# Abstract

This third report describes a new method to control single-link lumped-mass flexible arms in the case of having friction in the joint and changes in the payload. Both linear and nonlinear friction components are overcome by using the very robust control scheme developed in the second report, which is based on two nested feedback loops: an inner one that controls the motor position and an outer one that controls the tip position. In order to compensate for changes in the payload, an adaptive control scheme is used. Two cases are considered when compensating for changes in the tip payload: the arm is a minimum phase system or a non-minimum phase one. Different adaptive control schemes are proposed in each case. In them, compensation for changes in the load is achieved in two steps: first the tip payload is estimated from a very simple procedure proposed here, and then the feedforward and feedback controllers are tuned according to this estimated value. It results in a quite simple control law that can be used for real-time control of flexible arms, and that needs minimal computing effort. Experimental results are shown.

# 1. Introduction

Several methods have been developed during recent years to control single-link flexible arms with invariant parameters: [1-6], for example. These methods allow a precise control of the tip position by sensing some states of the motor and the tip (position, velocity, etc). All the states of the system are reconstructed from these measurements, and used to place the closed-loop poles of the arm. These reconstructions (by using filters or observers) usually involve a large amount of computation, especially when there is a high level of noise in the measurements.

A next step has been to consider that the parameters of the arm may vary with time. Some adaptive control schemes have been proposed to compensate for these changes. They are based on the methods mentioned in the previous paragraph and make use of the same sensing. The parameter that tipically has been considered to change is the tip payload ([7-10], e.g.), which represents the load carried by the robot. These adaptive controls are unnecessarily complicated to compensate for only one varying parameter. Moreover nonlinear and time varying joint frictions, which play important roles in many robots, are parameters that have not been considered in all these adaptive and non-adaptive methods [1-10].

This report is the third one of a series of reports that describe a new method to control single-link flexible arms. There are only two parameters that are likely to vary through the time in a flexible manipulator: the friction in the joint and the tip payload. We develop here a procedure to compensate for changes in these two parameters, that makes use of measurements at several points of the beam. We will show that the real time calculations carried out by the controller are dramatically reduced in our method, compared with the others. Our method is based on a feedforward-feedback combined scheme, and we particularize our study to the case of lumped-mass flexible arms. We showed in Report I that this method can be generalized to distributed-mass flexible arms by using the modelling technique described in Section 4 of this first report.

Lumped-mass flexible arms consist of massless flexible structures that carry masses concentrated at certain points of the beam (see Figure 1). Only translations of these masses produce stresses in the flexible structure, their rotations do not generate any torque in the beam. So the number of vibrational modes in the structure coincide with the number of lumped masses. Our control scheme makes use of measurement of the positions of all the lumped masses.

Problems caused by Coulomb friction (which is a nonlinear component of the friction) as well as for changes in the dynamic friction coefficient are overcome by using a general robust control scheme developed in [13] (Report II). This is composed of two nested loops: an inner loop that controls the motor position and an outer loop that controls the tip position. See Fig. 2, where $\theta_m$ is the motor angle, $\theta_n$ is the tip position angle, and $i$ is the motor current.

A new scheme is proposed to adapt the control law to changes in the load. Adaptive controls referenced above are based on the Model Reference Adaptive Control (*MRAC*) ([7], [8]); or on a two-stage process: a system identification stage followed by the adaptation of the controller as a function of the identified system parameters ([9], [10]). Both methods require a large amount of calculations to be performed in real-time. Then powerful computers have to be used, being problematic the use of these methods for control of multilink flexible arms. The adaptive control here proposed belongs to the second kind. But it estimates only the tip payload (instead of the whole dynamic model) and changes only some specific coefficients of the controllers. It makes the identification stage very fast and the adaptation law very simple.

The dynamic model of single-link flexible arms with lumped masses is resumed in Section 2. The control loop for the motor position is briefly described in Section 3. Section 4 describes the tip position control schemes used in both cases: minimum and non-minimum phase systems, when the tip payload is invariant. And Section 5 develops the corresponding adaptive schemes. Experimental results are shown in Section 6, and conclusions are stated in Section 7.

## 2. Lumped-Mass Flexible Arm Model

This section briefly resumes Section 2 of Part I. We divide the model of our flexible arm into two submodels: the first one describes the behavior of the motor, the second one describes the behavior of the mechanical structure using the angle of the motor as its input. These two submodels are coupled by the reaction torque of the beam on the motor. This model is quite different from the models normally used in control of flexible arms, which consider the applied torque as the input to the beam (Truckenbrodt [14], Low [15]). Our model has some advantages when identifying flexible arms with friction in the joints [16], and when trying to compensate for friction [13]. Another advantage of our model is that it allows us to separate the dynamic-model terms that depend on the geometry of the beam from the terms that depend on the lumped masses of the beam, facilitating the payload identification process.

Consider the system of Figure 1. It represents a massless flexible beam with $n$ point masses distributed along the structure, the last mass being located at the tip of the beam. The inertia of the motor is included in the motor submodel. Let $m_i, 1 \leq i \leq n$ be the values of the masses and $l_i$ the distances between consecutive masses $i-1$ and $i$, where $l_1$ is the distance between the rotation axis of the motor and the first mass. We assume that beam deflections are small enough so that the distances between masses $m_i$ (measured along length of beam) are equal to the distances between the masses' projections on $x$-axis.

We establish a coordinate system $\bar{x}-\bar{y}$, that is fixed in space with origin at the motor axis. We denote as $\theta_i$ the angle between $\bar{x}$-axis and the radial line from the origin to mass $i$ (see Figure 1). The angle of the motor is denoted $\theta_m$.

It can be shown [11] that the dynamic equation for this beam submodel is:

$$\mathcal{M} \cdot \frac{d^2\Theta}{dt^2} = E \cdot I \cdot [\mathcal{A} \cdot \Theta + \mathcal{B} \cdot \theta_m] \tag{1}$$

where $\mathcal{M} = diag(m_1, m_2, \ldots, m_n), \Theta^T = (\theta_1, \theta_2, \ldots, \theta_n)$ is the vector of beam measured positions, $\mathcal{A}$ is an $n \times n$ constant matrix, $\mathcal{B}$ is a constant $n \times 1$ column vector, and $E \cdot I$ is the stiffness of the beam, which is assumed constant through the beam. In this expression, $\mathcal{A}$ and $\mathcal{B}$ depend only on the geometry of the beam: $l_i$. The values of the lumped masses influence only matrix $\mathcal{M}$.

The dynamic equation for the DC motor submodel is very simple:

$$K \cdot i = J \cdot \frac{d^2\theta_m}{dt^2} + V \cdot \frac{d\theta_m}{dt} + C_t + CF \tag{2}$$

where $K$ is the electromechanical constant of the motor, $i$ is the current, $J$ is the polar inertia of the motor, $V$ is the dynamic friction coefficient, $C_t$ is the coupling torque between motor and beam and $CF$ is the Coulomb friction.

We can express the coupling torque as a linear function [11]:

$$C_t = \mathcal{H} \cdot \Theta + h_{n+1} \cdot \theta_m \tag{3}$$

where $\mathcal{H} = (h_1, h_2, \ldots, h_n)$; $h_i, 1 \leq i \leq n+1$ are parameters that do not depend on the masses of the beam.

## 3. Motor Position Control Loop

We resume here Section 3 of Part II. This control loop corresponds to the inner loop of Figure 2. We want to achieve two objectives when designing a controller for this loop:

1. to remove the modeling error and the nonlinearities introduced by Coulomb friction and changes in the coefficient of the dynamic friction,
2. to make the position controlled response of the motor much faster than the response of the tip position control loop (outer loop in Figure 2).

The fulfillment of the second objective will allow us to substitute for the inner loop, an equivalent block whose transfer function is approximately equal to one; i.e. the error in motor position is small and quickly removed. This simplifies the design of the outer loop as will be seen in the next section.

To simplify the design of the inner loop, the motor submodel described in equation (2) can be linearized by compensating for the Coulomb friction and can be decoupled from the dynamics of the beam by compensating for the coupling torque. This is done by adding to the control current, the current equivalent to these torques which is given by

$$i_c(t) = (C_t(t) \pm CF)/K \tag{4}$$

where the sign of $CF$ coincides with the sign of the motor velocity.

The coupling torque $C_t(t)$ can be calculated either from strain gauge measurements at the base of the link, or can be estimated, by using expression (3), from position measurements of the lumped masses and the motor angle. The second approach is used here. After compensating for the friction and coupling torque, the transfer function between the angle of the motor and the current is given by

$$\frac{\theta_m(s)}{i(s)} = M(s) = \frac{K/J}{s \cdot (s + V/J)}. \tag{5}$$

The block diagram of the inner loop control system is shown in Figure 3 (discrete controllers version). The feedforward and feedback controllers ($A(z)$ and $B(z)$ respectively) are designed so that the response of the inner loop (motor-position-control) is significantly faster than the response of the outer loop (tip-position-control) and without any overshoot. This is done by making the gain of the feedforward controller large. It was shown in [13] that, in theory, this gain could be made arbitrarily large even in the case of the arm being a non-minimum phase system. It was shown also that large gains in this loop reduce the effects of nonlinearities because of friction. Practical limits to these gains are given by the saturation

current of the D.C. motor amplifier, unmodelled high frequency dynamics, or even unstability because of the discretization of the signals when using digital controllers.

When the closed-loop gain of the inner loop is sufficiently high, the motor position will track the reference position with small error. Then the dynamics of the inner loop may be approximated by 1 when designing the outer loop controller.

Notice that the dynamics of this inner loop is independent of the payload, so controllers of Figure 3 do not have to be adaptively tuned. This is because the only dependence of this submodel on the payload is through the coupling torque, and it is exactly compensated by using position measurements and expression (3), whose parameters $h_i$ are independent of the payload.

# 4. Nonadaptive Tip Position Controller

Provided that the inner loop has been satisfactorily closed, the dynamics of the arm are reduced to the dynamics of the beam submodel. Because the transfer function of the inner loop is approximately 1, then $\theta_{mr} \simeq \theta_m$. We assume in what follows that both variables are identical.

The transfer function between the tip and motor positions is given by:

$$\frac{\theta_n(s)}{\theta_m(s)} = g_n(s) = C_n \cdot (\mathcal{M} \cdot s^2 - E \cdot I \cdot A)^{-1} \cdot E \cdot I \cdot B \tag{6}$$

where $C_i = \begin{pmatrix} 0 \ldots 010 \ldots 0 \end{pmatrix}$ the 1 being in the $i-th$ column. This transfer function holds for the case where tip payload is constant.

If $g_n(s)$ is minimum phase, the simple control scheme described in Subsection 4.1 may be used. If it is non-minimum phase, a general control scheme is proposed in Subsection 4.2. In general, the controller for the tip position is composed of a combined feedforward/feedback control law. The feedforward component is responsible of driving the tip of the arm closely to the desired trajectory, and the feedback term is responsible of correcting tracking errors.

## 4.1. Control of minimum phase arms

The control scheme proposed here exploits the particular structure of equation (1). If we close a loop using a feedback law of the form:

$$\theta_{mr}(t) = (C_n \cdot B)^{-1} \cdot [\eta(t) - C_n \cdot A \cdot \Theta(t)], \tag{7}$$

we transform equation (6) into the simple expression:

$$\frac{\theta_n(s)}{\eta(s)} = \frac{E \cdot I / m_n}{s^2}. \tag{8}$$

Equation (8) corresponds to the dynamics of a rigid single-link arm, and techniques to control this are well known. We propose the scheme of Figure 4 to drive the arm using second order parabolic profiles as trajectories for the tip. The feedforward term provides with the acceleration of the desired trajectory, and the feedback term is a standard *P.D.* controller that corrects tip position errors.

Notice that the feedback law (7) cancels all the zeros of the plant (and all the poles but two). It means that, if the system has zeros in the right half-plane, some intermediate $\theta_i, i \neq n$, and $\theta_m$ become unstable. Therefore, this scheme cannot be used for non-minimum phase flexible arms, and a more general method is needed.

### 4.2. General control scheme

A general control scheme is proposed here, that may be used for both minimum and non-minimum phase systems (see Figure 5). But now the controller for the tip position is more complicated.

#### *4.2.1. Feedforward term*

If the transfer function between the angle of the motor and the angle of the tip $g_n(s)$ is minimum phase, then a second order parabolic profile can be used and the feedforward term is $g_n^{-1}(s)$. But if this transfer function is non-minimum phase, then a quasi-parabolic profile with derivatives bounded up to the fourth order (see Fig. 6) is used in order to guarantee the implementability of the feedforward term, and the nominal quasi-parabolic profile is passed through a special filter in order to avoid unbounded control signals. We denote that nominal trajectory as $P_p$.

The necessity of the above mentioned filter is justified from Figure 7. Assume an open loop control for the case without external perturbations. If we want the tip to follow the reference exactly, then the control signal $\hat{\theta}_{mr}$ (which is the same as $\theta_m$ neglecting the dynamics of the inner loop) is obtained by passing the desired profile $P_p$ through a block $\hat{g}_n(s)$ that implements the inverse of the plant $g_n(s)$. If this plant had zeros in the right half-plane, they would become unstable poles in $g_n^{-1}(s)$ producing an unbounded $\hat{\theta}_{mr}$ control signal. In order to avoid this, a modified $\hat{g}_n(s)$ term must be used and the tip reference would be now:

$$\theta_{nr}(s) = g_n(s) \cdot \hat{g}_n(s) \cdot P_p(s) \tag{9}$$

$P_p(s)$ being the Laplace transform of the parabolic or quasi-parabolic profile. This filter is chosen in such a way to get a reference trajectory $\theta_{nr}$ as close as possible to the desired reference $P_p$, taking into account the constraint of a bounded $\hat{\theta}_{mr}$. We choose as a representative index of the closeness between trajectories the integral of the squared difference between both profiles (see Fig. 7):

$$\mathcal{J} = \int_0^\infty e^2(t) \cdot dt = \frac{1}{2 \cdot \pi \cdot j} \int_{-j\infty}^{j\infty} \frac{2}{s^3} \cdot (1 - g_n(s) \cdot \hat{g}_n(s)) \cdot \frac{2}{-s^3} \cdot (1 - g_n(-s) \cdot \hat{g}_n(-s)) \cdot ds \tag{10}$$

where a parabolic profile $2/s^3$ has been assumed for $P_p$ because, from Figure 6, the quasi-parabolic profile behaves as a parabolic one most of the time, being a 4-th order parabola only at the short transitions from maximum to minimum acceleration and vice versa.

Assuming that $g_n(s)$ is of the form:

$$g_n(s) = \bar{K} \cdot \frac{\prod_{i=1}^{n_1}(s - a_i) \cdot \prod_{j=1}^{n_2}(s - b_j)}{d(s)}$$

where $a_i < 0, 1 \leq i \leq n_1; b_j > 0, 1 \leq j \leq n_2$, and all the roots of $d(s)$ are in the left half-plane, it can be shown [12],[17] that the optimum $\hat{g}_n(s)$ that minimizes the cost defined in (10) is given by

$$\hat{g}_n(s) = \frac{d(s) \cdot (\alpha_2 \cdot s^2 + \alpha_1 \cdot s + \alpha_0)}{\bar{K} \cdot \prod_{i=1}^{n_1}(s - a_i) \cdot \prod_{j=1}^{n_2}(s + b_j)} \tag{11}$$

where the $\alpha$ coefficients are obtained from the partial fraction expansion of $\frac{\prod_{j=1}^{n_2}(s + b_j)}{s^3 \cdot \prod_{j=1}^{n_2}(s - b_j)}$, $\alpha_0, \alpha_1, \alpha_2$ being the coefficients corresponding to the terms whose denominators are $s, s^2, s^3$ respectively. The filter is then

$$g_n(s) \cdot \hat{g}_n(s) = (\alpha_2 \cdot s^2 + \alpha_1 \cdot s + \alpha_0) \cdot \frac{\prod_{j=1}^{n_2}(s - b_j)}{\prod_{j=1}^{n_2}(s + b_j)} \tag{12}$$

*4.2.2. Feedback term*

The feedback controller is designed using optimization techniques (e.g. [18]). We design a controller: $\gamma(s) = -\Lambda \cdot x(t)$ that drives $x$ from an initial state to the zero state minimizing a cost function of the form:

$$\mathcal{J} = \int_{t=0}^{\infty} (x^T(t) \cdot R_1 \cdot x(t) + R_2 \cdot \theta_{mr}^2(t)) \cdot dt \tag{13}$$

where $R_1 \in \Re^{2 \cdot n \times 2 \cdot n}, R_2 \in \Re$ are weighting matrices, and $x \in \Re^{2 \cdot n}$ is the state vector of the system. We get from (1) the state equation of the system:

$$\dot{x}(t) = \begin{pmatrix} 0 & I_n \\ E \cdot I \cdot \mathcal{M}^{-1} \cdot \mathcal{A} & 0 \end{pmatrix} \cdot x(t) + \begin{pmatrix} 0 \\ E \cdot I \cdot \mathcal{M}^{-1} \cdot \mathcal{B} \end{pmatrix} \cdot \theta_m(t) \tag{14}$$

where $x^T(t) = \begin{pmatrix} \Theta^T & \dot{\Theta}^T \end{pmatrix}$, and $I_n \in \Re^{n \times n}$ is the identity matrix.

This feedback scheme uses the errors between the desired and the actual states to generate the control signal. Defining $\Lambda = \begin{pmatrix} \Lambda_1 & \Lambda_2 \end{pmatrix}$; $\Lambda_1, \Lambda_2 \in \Re^{1 \times n}$ we can express the control signal ($\gamma$) in function of the measured variables: $\gamma(s) = (\Lambda_1 + \Lambda_2 \cdot s) \cdot (\Theta_r(s) - \Theta(s))$.

The reference vector for the measured variables ($\Theta_r$) may be obtained from the reference $\theta_{nr}$ by using the following expression derived from (1):

$$\Theta_r(s) = \Upsilon(s) \cdot \theta_{nr}(s), \tag{15}$$

$$\Upsilon(s) = \begin{pmatrix} C_1.Adj(\mathcal{M} \cdot s^2 - E \cdot I \cdot \mathcal{A}) \cdot E \cdot I \cdot \mathcal{B} \\ C_2.Adj(\mathcal{M} \cdot s^2 - E \cdot I \cdot \mathcal{A}) \cdot E \cdot I \cdot \mathcal{B} \\ \vdots \\ C_n.Adj(\mathcal{M} \cdot s^2 - E \cdot I \cdot \mathcal{A}) \cdot E \cdot I \cdot \mathcal{B} \end{pmatrix} \cdot \frac{1}{C_n.Adj(\mathcal{M} \cdot s^2 - E \cdot I \cdot \mathcal{A}) \cdot E \cdot I \cdot \mathcal{B}} \tag{16}$$

In the case of a non-minimum phase system, the denominator of this expression has some positive real component roots. But they are cancelled with the zeros of filter (12), leaving $\Theta_r(t)$ bounded. Cancellation may be exactly done because all these terms are computed.

This feedback control scheme presents important advantages over other existing schemes when implemented on a digital computer. Other control methods need to reconstruct the whole state $x$ from measurements of the motor and tip of the arm by means of filters or observers. They involve a large amount of computation. Also, in many cases, these reconstructions are distorted by the noise of the measured signals making the control difficult. But in our case, because a) we have simplified the arm dynamics by closing the motor position loop, and b) we are using more sensing in the beam, all the states may be easily obtained: positions are measured and velocities may be approximated by the simple difference equation

$$\dot{\Theta}(k \cdot T) = (\Theta(k \cdot T) - \Theta((k-1) \cdot T))/T \tag{17}$$

where $T$ is the sampling period and $k$ is an integer. Because only the first derivative of measured signals is needed, this approximation of the velocities of the mass points is reasonable in many cases, even having relatively high levels of measurement noise.

## 5. Adaptive Tip Position Controller

The adaptive control is composed of two stages: the first one identifies the tip mass, and the second tunes the coefficients of the controllers as functions of the estimated values of the masses.

### 5.1. Payload Estimation

We assume that changes in the tip payload are caused by the weight of the different objects carried by the manipulator. Then we assume that the tip payload remains constant during each movement.

Lumped masses of our arms may be easily estimated by three ways from equation (1):

1. by double differentiation of $\theta_n(t)$:

$$m_n = \frac{E \cdot I \cdot [C_n \cdot \mathcal{A} \cdot \Theta + C_n \cdot \mathcal{B} \cdot \theta_m]}{d^2\theta_n/dt^2}. \tag{18}$$

2. by integrating twice equation (1):

$$m_n = \frac{E \cdot I \cdot \int_{\tau_2=0}^{t} \int_{\tau_1=0}^{\tau_2} [C_n \cdot \mathcal{A} \cdot \Theta(\tau_1) + C_n \cdot \mathcal{B} \cdot \theta_m(\tau_1)] \cdot d\tau_1 \cdot d\tau_2}{\theta_n(t)} \tag{19}$$

3. and by using the solution intermediate between the previous two: differentiating once the left-hand term and integrating once the right-hand term of equation (1).

Notice that we can use these expressions because of the property that matrices $A,B$ *are independent of the tip mass* $m_n$. Any of these estimators may be used. The selection will depend on the quality of the measurements. Expression (19) seems to be the most adequate because no derivatives of the tip position measurement are required; then noisy measurements may be used to estimate $m_n$. But, in turn, this estimator carries out a double integration, and it showed to be very sensitive to little permanent errors in the position measurements due to errors in the calibration of the arm or permanent bendings of the beam.

Finally, we assumed that $m_n$ is the only mass that can change. Provided that we know the values of masses $1 \leq i < n$, we can use equation (1) to obtain the accelerations of these masses, and they can be used to get better estimations of states $\dot{\theta}_i, 1 \leq i < n$ than ones obtained from (17). The trajectory described by the tip is often the slowest one among the trajectories of all the points of the beam. Then relatively good estimations may be achieved for $\dot{\theta}_n$ from (17).

### 5.2. Tuning the Controllers

No controller of the motor position control loop needs to be tuned, because the decoupling term is independent of the payload. Only the parameters of the tip position control loop need to be tuned as described below.

#### *5.2.1. Minimum phase controller*

The feedback law (7) is independent of the tip mass. Only the gain $m_n/EI$ of Figure 4 needs to be tuned as a function of the estimated mass. This tuning keeps all the performances of this control scheme unchanged.

#### *5.2.2. General scheme*

Analyzing the controllers of Figure 5 we get [12]:

- $g_n(s) \cdot \hat{g}_n(s)$ is independent of $m_n$.

- Only numerators of $\hat{g}_n(s)$ and $\Upsilon(s)$ depend on $m_n$.
- If we consider a perturbation $\varepsilon(s)$ applied to the input of the system ($\theta_m$), then the resulting closed-loop transfer function is

$$\frac{\theta_n(s)}{\varepsilon(s)} = \frac{g_n(s)}{1 + g_n(s) \cdot (\Lambda_1 + \Lambda_2 \cdot s) \cdot \Upsilon(s)} \tag{20}$$

  and the zeros of this transfer function do not depend on the tip payload or on the coefficients of the controller.

All this means that few computations are needed to tune the controller to the new estimated payload:

- The feedforward term $\hat{\theta}_{mr}$ may always be expressed as:

$$\hat{\theta}_{mr}(t) = \hat{\theta}'_{mr}(t) + m_n \cdot \hat{\theta}''_{mr}(t), \tag{21}$$

  where $\hat{\theta}'_{mr}, \hat{\theta}''_{mr}$ are functions independent of $m_n$. These functions can be easily generated from (11), taking into account that the term

$$\frac{\alpha_2 \cdot s^2 + \alpha_1 \cdot s + \alpha_0}{\prod_{i=1}^{n_1}(s - a_i) \cdot \prod_{j=1}^{n_2}(s + b_j)}$$

  is independent of the payload, and can be implemented as a filter whose transfer function has constant coefficients. The only term that depends on the payload is the factor of the numerator $d(s)/\bar{K}$. This polynomial has coefficients that are proportional to $m_n$, and others that are independent of this mass. Grouping the coefficients that are independent of $m_n$ and multiplying them by the previous filter and the Laplace transform of the reference signal $P_p$, we get $\hat{\theta}'_{mr}(t)$. $\hat{\theta}''_{mr}(t)$ is obtained in a similar way from those coefficients of $d(s)/\bar{K}$ that depend on $m_n$.
- The reference $\Theta_r$ may be expressed in a form similar to the previous:

$$\hat{\Theta}_r(t) = \hat{\Theta}'_r(t) + m_n \cdot \hat{\Theta}''_r(t). \tag{22}$$

- Controller $\Lambda_1 + \Lambda_2 \cdot s$ has to be adjusted in order to maintain the poles of the closed-loop system (20) in the same positions. This is an algebraic procedure that involves resolving a system of linear equations. Often, only the dominant poles have to be placed. This significantly reduces the amount of calculations.

Figure 8 shows this tip position adaptive control scheme.

## 6. Experimental Results

In this section we apply the methods described in this paper to control two single-link lumped-mass

flexible arms that we have built in our laboratory. The experimental setup is described first. Then experimental results are presented for our two arms, which correspond to the single and two mass cases. The single-mass arm is minimum phase and the two-mass arm is non-minimum phase. Then the two methods presented in this paper are applied.

### 6.1. Single-mass flexible arm

From an identification technique described in [11], [16] we found that the parameters of this arm were:

$J = 0.005529\ lb.in.sec^2$
$V = 0.01216\ lb.in./rad./sec.$
$K = 2.184\ lb.in./amp.$
Coulomb friction = 0.2883 *lb.inch* (0.132 *amp.*)

$$C_t(t) = C \cdot (\theta_m - \theta_1), \quad C = 0.674 lb.in./rad.. \tag{23}$$

Equation (1):

$$54 \cdot s^2 \cdot \theta_1(s) = -2362.5 \cdot \theta_1(s) + 2362.5 \cdot \theta_m(s), \tag{24}$$

and

$$g_1(s) = \frac{43.75}{s^2 + 43.75} \tag{25}$$

The estimated value of the Coulomb friction corresponds to the equivalent torque generated by a beam deflection of 25 degrees, so its effect in the control is very noticeable. Transfer function (25) is minimum phase. Then we use the control scheme of Subsection 4.1.

#### *6.1.1. Design of inner control loop*

The inner loop incorporates compensation terms for the Coulomb friction and the coupling between the motor and the beam, according to (2). The scheme of Figure 3 is used for the inner loop. A delay term is included in the scheme in order to take into account the delay in the control signal because of the computations. A sampling period of 3 *msec.* is used for this inner loop.

An optimization program was developed to get the best controllers using the model obtained for the motor. The settling time (considering an error less than 1 %) of the response of the motor to step commands in the motor angle reference input was minimized. The saturation limit of the current amplifier was taken into account in this design too. Step inputs were assumed as references for the inner loop because, in order to get a good control action, the command angle for the motor should experience very sharp changes. In fact in our experiments the motor angle varied much faster than the angle of the tip.

The resulting controllers were:

$$A(z) = 17.442 - 2.442 \cdot z^{-1}$$

$$B(z) = 6.667 - 5.667 \cdot z^{-1}$$

This motor position closed loop proved to be fast and accurate enough to assume that the dynamics of this inner loop are negligible compared to the dynamics of the beam. Details may be found in [19].

*6.1.2. Design of outer control loop*

Notice that matrices $A$ and $B$ of (24) include the constant term $E \cdot I$. Because this system is minimum phase, we use the method of Subsection 4.1. First we close the loop (7):

$$\theta_{mr}(t) = \frac{\eta(t)}{2362.5} - \theta_m(t). \tag{26}$$

Then we design the controller $G_c(z)$ of Figure 4. Designing an analog *P.D.* controller and then discretizing it using the Tustin transform (e.g. [20]) we get the digital controller:

$$G_c(z) = 3281.25 \cdot \frac{1 - 0.987 \cdot z^{-1}}{1 - 0.74 \cdot z^{-1}} \tag{27}$$

*6.1.3. Adaptation*

Identification of the tip mass is done by using (19) [19]. The complete control scheme is shown in Figure 10. Experimental results are shown in Figures 11-14. Parabolic profiles of order 2 are given to the controller as references for the tip position. Comparisons between the behavior of the arm when using the nominal controller (27) ($m_n$ = 54 *gms.* in the block $m_n/EI$ of Figure 4) and when using the adaptive controller (block $m_n$ is tuned) are presented. Figure 11 shows the response of the system with the nominal payload of 54 *gms.* and the nominal controller (non-adaptive). Notice that the response is very good because $G_c$ was designed for these conditions. Figure 12 shows the adaptive response with the nominal payload. Figure 13 shows both adaptive and non-adaptive responses when payload is 142 *gms.*, and Figure 14 when the payload is 15.73 *gms.* Notice that the system without the adaptive controller becomes unstable in this last case.

### 6.2. Two-mass flexible arm

The motor submodel is the same here as in the previous arm, because we use the same motor. Coupling torque is now:

$$C_t(t) = -6.159 \cdot \theta_1(t) + 2.053 \cdot \theta_2(t) + 4.106 \cdot \theta_m(t), \tag{28}$$

and the beam submodel is, assuming the two nominal masses of 54 *gms* (0.12136 *lb.*):

$$\begin{pmatrix} 0.12136 & 0 \\ 0 & 0.12136 \end{pmatrix} \cdot \frac{d^2\Theta(t)}{dt^2} = \begin{pmatrix} -176.6032 & 110.377 \\ 27.59425 & -22.0754 \end{pmatrix} \cdot \Theta(t) + \begin{pmatrix} 66.2262 \\ -5.51885 \end{pmatrix} \cdot \theta_m(t). \quad (29)$$

This last expression gives the transfer functions:

$$\frac{\theta_1(s)}{\theta_m(s)} = \frac{545.7 \cdot (s^2 + 106.10833)}{s^4 + 1637.1 \cdot s^2 + 57903.3175} \quad (30)$$

$$\frac{\theta_2(s)}{\theta_m(s)} = \frac{-45.465 \cdot (s^2 - 1273.3)}{s^4 + 1637.1 \cdot s^2 + 57903.3175} \quad (31)$$

Natural frequencies of the beam are obtained from the poles of these transfer functions. They are: 6.014 *rad./sec.* and 40.0116 *rad./sec.*. The last transfer function is non-minimum phase exhibiting a positive zero placed at 35.683. Then the general control mehod of Subsection 4.2 is used here.

### *6.2.1. Motor position control loop*

Because we use the same motor as in the previous arm, we use the same controllers for the inner loop too. Only the compensation term of the motor-beam coupling has to be changed. This is implemented by using expression (28). We continue here using a sampling period of 3 *msec*. Experiments showed that the dynamics of the motor position inner loop were negligible [12] using this controller.

### *6.2.2. Outer loop*

We use a sampling period of 6 *msec.* for this loop. We want to test the tuning of both feedforward and feedback controllers. Then, in this experiment, in order to separate the results of tuning these two terms, we drive the system open loop along a trajectory (only the feedforward term works). In turn, when the arm is resting in a position, only the feedback term works to compensate for external perturbations.

Figure 15 shows the tip position reference $\theta_{mr}$ that results from passing the fourth order parabolic profile $P_p$ through filter (12). The arm has to move 200 *mrad.* in about 0.4 *sec.*. The components of the feedforward term, expressed according to (21), are:

$$\hat{\theta}'_{mr}(s) = \frac{(852.81575 + 2.6791 \cdot s^2) \cdot (1 + 0.05605 \cdot s + 0.00157075 \cdot s^2)}{0.6697676 \cdot (s + 35.6833)^2} \cdot P_p(s) \quad (32)$$

$$\hat{\theta}''_{mr}(s) = \frac{s^2 \cdot (176.6032 + 0.12136 \cdot s^2) \cdot (1 + 0.05605 \cdot s + 0.00157075 \cdot s^2)}{0.6697676 \cdot (s + 35.6833)^2} \cdot P_p(s), \quad (33)$$

as shown in Figure 16. Notice that $\lim_{t\to\infty} \hat{\theta}'_{mr}(t)$ = desired tip position, and $\lim_{t\to\infty} \hat{\theta}''_{mr}(t) = 0$. So the steady

state of the feedforward term is not affected by changes in the tip load. Because we move the arm under open loop control conditions, we do not need $\Upsilon$.

In order to get the feedback controller, we chose a cost function (13) of the form: $R_1 = diag(1,2,0,0)$, $R_2 = 1$, where we weighted the tip position twice the middle mass and motor positions. The optimum controller that minimizes this cost is:

$$\Lambda = \begin{pmatrix} 0.4428 & 0.5572 & 0.0534 & 0.1828 \end{pmatrix}. \tag{34}$$

This places the closed-loop poles at $-3.79 \pm j \cdot 7.375, -6.61 \pm j \cdot 40.506$. There are two dominant poles and two secondary poles far away from them.

*6.2.3. Adaptation*

**Identification** We first tried to estimate the tip mass by using expression (19), like in the first example. But the problem mentioned in Subsection 5.1 appeared. Experimentation showed that (18) was the best estimation among the three proposed there. Measurements of Selspot are very noisy so we had to pass all $\theta_i$ measurements through a low pass filter with cut off frequency 100 *rad./sec.*

The tip acceleration was estimated by fitting a second order parabola to several consecutive tip position samples. At the first instants of the motion, tip position experiences little changes: first it moves slightly backwards and then it moves forward at a low speed. Then the tip acceleration is close to 0 and estimations based on (18) are unreliable. Estimations are consistent after about 0.15 *sec.* from the start of the movement, when the tip experiences noticeable motion.

**Controller adjustment** Analysis showed that both dominant and secondary poles of the closed loop system could be maintained approximately in the same positions (deviations less than 20% with respect to the values given at the end of the outer loop design subsection), for variations of the payload between 30 *grams* and 160 *grams*, by tuning independently the *P.D.* controllers associated with each mass position measurement. Further analysis showed that good results are attained by using the following simple adaptive law:

$$\lambda_i' = \rho \cdot (1 + \lambda_i) - 1 \tag{35}$$

$$\lambda_j' = \rho \cdot \lambda_j, \tag{36}$$

where $\lambda_i, i = 1,2$ are the two first elements of vector $\Lambda$ (position coefficients), and $\lambda_j, j = 3,4$ are the two last elements of this vector (velocity coefficients); $\lambda$ represents the coefficients of the controller for the nominal tip mass $m_n$, and $\lambda'$ represents the coefficients of the new *P.D.* controller for the estimated new tip mass $m_n'$; and $\rho$ is $m_n'/m_n$.

An adaptive controller based on the above ideas would run the first 0.15 *sec.* of the motion (where the tip mass is being identified) with the nominal controller, and the remaining of the motion with the

tuned controller. This works in minimum phase systems, where the gains of the feedback controller are high (single-mass case) and allow the system to recover from the position errors produced during these 0.15 *sec*. But in non-minimum phase systems, feedback gains have to be low (in order to have a stable closed loop system), and tracking errors produced in these first 0.15 *sec*. cannot be corrected during the remaining 0.25 *sec*. of motion, the trajectory described by the tip being quite distorted.

Then, the following experiment was designed to test open and closed loop performances in our two-mass arm. The experiment is composed of four phases (see Figure 17). The first two phases are needed for the identification of the tip mass. The other two correspond to the real movement of the arm, with the controller coefficients already tuned. They are:

**Phase 1** The arm is open loop driven (inner loop is closed, outer loop is open) following the trajectory $\theta_{mr}$ obtained from a Quasi-parabolic profile $P_p$. The feedforward signal is generated from (32), (33) assuming the nominal tip mass of 54 *gms*. We are estimating the tip mass during all this phase. The arm is driven in this way until we get a consistent estimation of $m_n$ (until about 0.15 *sec*.).

**Phase 2** Once the tip mass has been estimated, the feedback controller is recalculated according to (35), (36), the open loop control is stopped, the new feedback loop is closed, and the tip reference is settled to the initial position. Then the arm goes back to the initial state.

**Phase 3** Once the arm is approximately in the initial state, we start the real motion. In this phase we drive the arm according to the nominal trajectory by using the open loop controller. The feedforward controller has already been tuned ((21) with the value of the estimated tip mass), so the tip position reference is closely tracked.

**Phase 4** Finally, when the tip has approximately reached the goal position, the controller is switched from an open to a closed loop scheme. In this phase, the work is carried out by the tuned feedback controller, that positions the tip exactly on the target position, and compensates for external perturbations.

Figure 17 shows the tip reference, and tip position obtained for a tip mass of 54 *gms*. (the nominal value). The value given by the estimator was 58 *gms*. Figure 18 shows that the commanded position for the motor ($\theta_{mr}$) is closely tracked by the actual motor position ($\theta_m$), supporting the assumption that the dynamics of the inner loop are of secondary order compared to the dynamics of the beam. Figure 19 shows the results of repeating the experiment with a tip mass of 133 *gms*. The estimated mass was now 120 *gms*. Figure 20 shows the response of the arm, with a tip mass of 133 *gms*., when the nominal controller (34) is used without any adaptation.

Phase 2 is the most critical part of this process in the sense that is the longest one, and can cause oscillations. The arm experiences a strong acceleration in the direction opposite to the motion, and then a quick decceleration in order to be placed at the initial position. In some cases, it produces oscillations (see Figure 19) that are the result of saturating the amplifier. These phenomena do not appear later, in phase 4, where the feedback loop is working again, under less extreme conditions.

## 7. Conclusions

A new method to control single-link lightweight flexible arms in the presence of joint friction and changes in the load has been presented.

Reduction of frictional nonlinear effects is achieved by closing a high gain loop around the motor position. This was developed in a previous paper [13] (and Report II) and includes compensating terms for the coupling torque and the Coulomb friction.

The new ideas that this report presents are two schemes to control the tip position of the arm when there are changes in the tip load. The first scheme is significantly simpler than the second, but can be used only in minimum phase systems.

The general control scheme (second one) is shown to be simple and computationally efficient: the sampling period was 3 *msec.* in our experiments and this was the time needed by real-time control calculations. The controller is composed of two nested control loops (three in the first scheme) plus an adaptation loop, but each one is formed by very simple elements. In fact, our experiments show that using a computer of very modest calculation capabilities, a controller that fulfills the desired specifications can be implemented. The experimental responses were shown to be good even in the case of extreme conditions: the Coulomb friction was very high and the payload ranged from 1/3 to 3 times the nominal tip load of 54 gr..

Experimental results showed that our control scheme made the tip follow the reference accurately even with a 10% error in the estimates of the tip mass, as happened in our experiments.

Phase 2 of the two-mass flexible arm experiment makes the total time required for the motion be unnecessarily large. In a practical implementation of this, Phase 2, returning tip to initial position, could be eliminated. Then tip would start from some new initial state closer to the goal state, and an appropiate new trajectory would have to be calculated. It means that the desired trajectory $\theta_{mr}$ and the feedforward signal $\hat{\theta}_{mr}$ should have to be recalculated at the end of Phase 1. These trajectories have to reach the final position, but now starting from the actual state of the arm, at the end of Phase 1, where the tip has some velocity, acceleration and, eventually, some jerk. Efficient ways of calculating these trajectories in order to avoid Phase 2 are object of our present research.

A significant advantage, from the design point of view, of our control scheme is that each loop is designed independently of the others (starting from the inner one) and their elements are calculated easily and according to simple specifications. The inner loop is designed to compensate friction and make the motor response fast. Both goals are achieved with the same high gain *P.D.* controller. The middle loop of the first scheme dramatically simplifies the dynamics of the system (reduces its transfer function to a double integrator). The outer loop wants a fast and accurate response in the tip position (a simple *P.D.* with a feedforward term). The adaptive control takes care of changes in the load by estimating only one parameter of the system; and Subsection 5.2 shows that the control scheme may be tuned to the new tip load with a minimum computation effort.

Finally, this control approach is different from others in the following sense. Existing methods to control flexible arms are based on the explicit control of the tip position only, where the controller generates the current for the DC motor of the joint as a control signal. The proposed method is based on the simultaneous explicit control of the joint motor position and tip position. The controller for the motor position generates a control signal that is a current for the DC motor, as in the other methods. But the tip position controller generates a control signal which is a motor position reference for the inner loop.

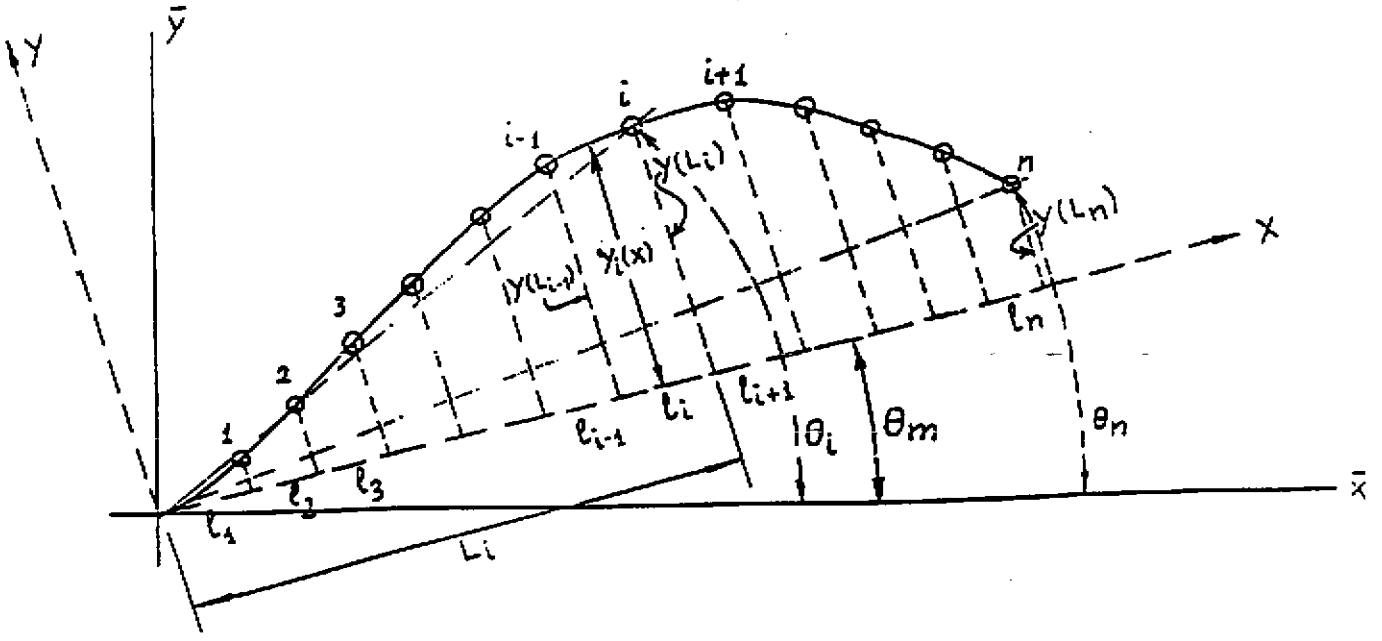


**Figure 1:** Lumped-mass flexible beam.

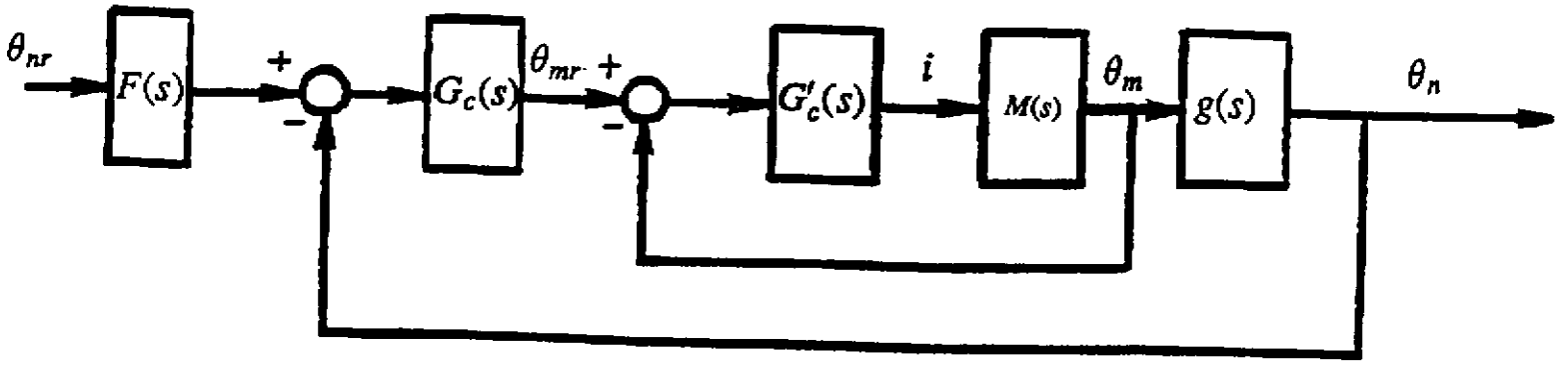


**Figure 2:** Control scheme robust to friction.

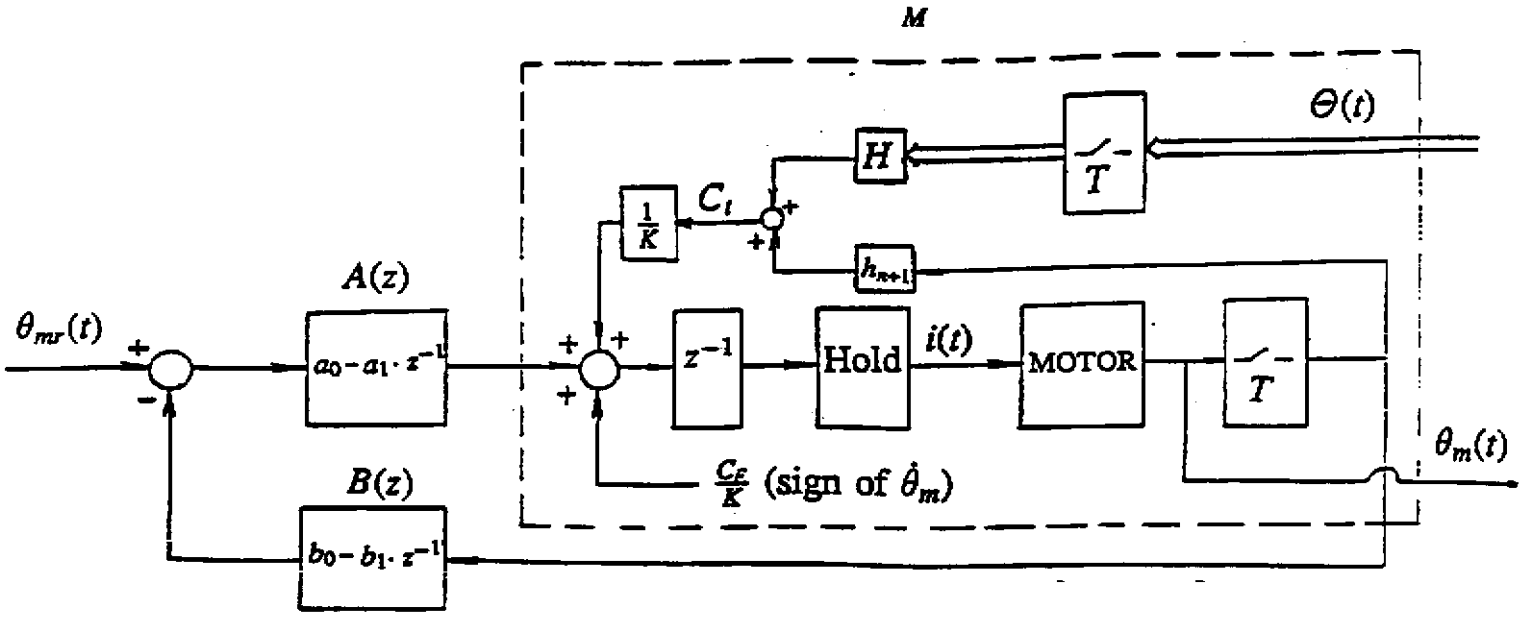


Figure 3: Computer control loop of the motor position.

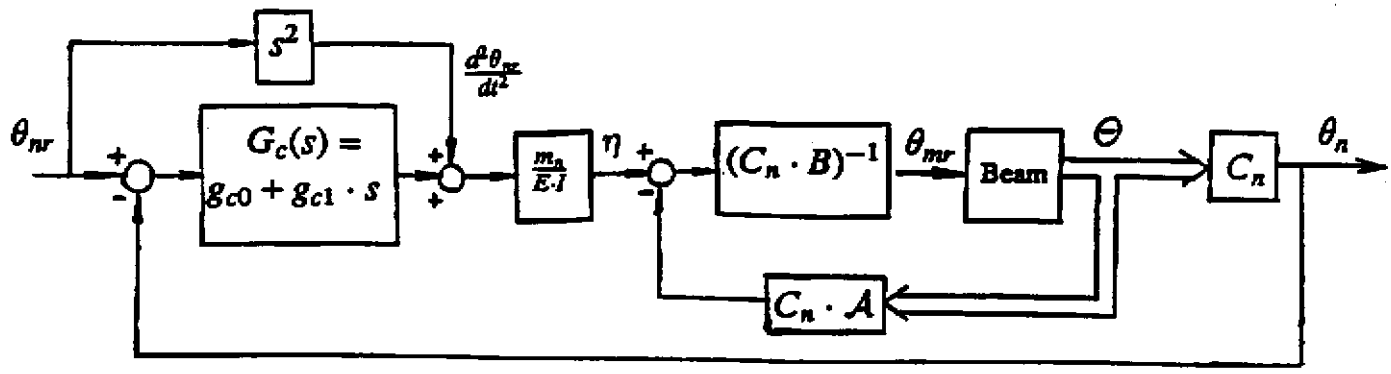


Figure 4: Tip position control scheme for minimum phase systems.

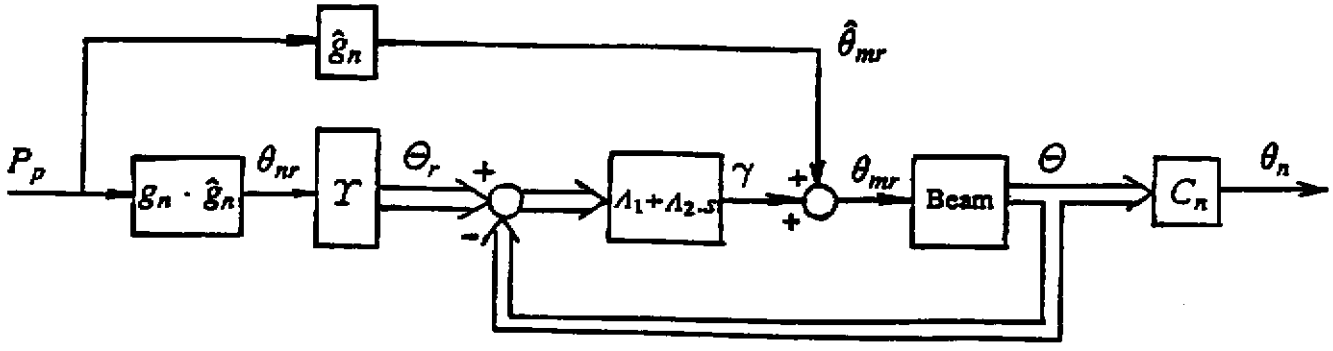


Figure 5: General tip position control scheme.

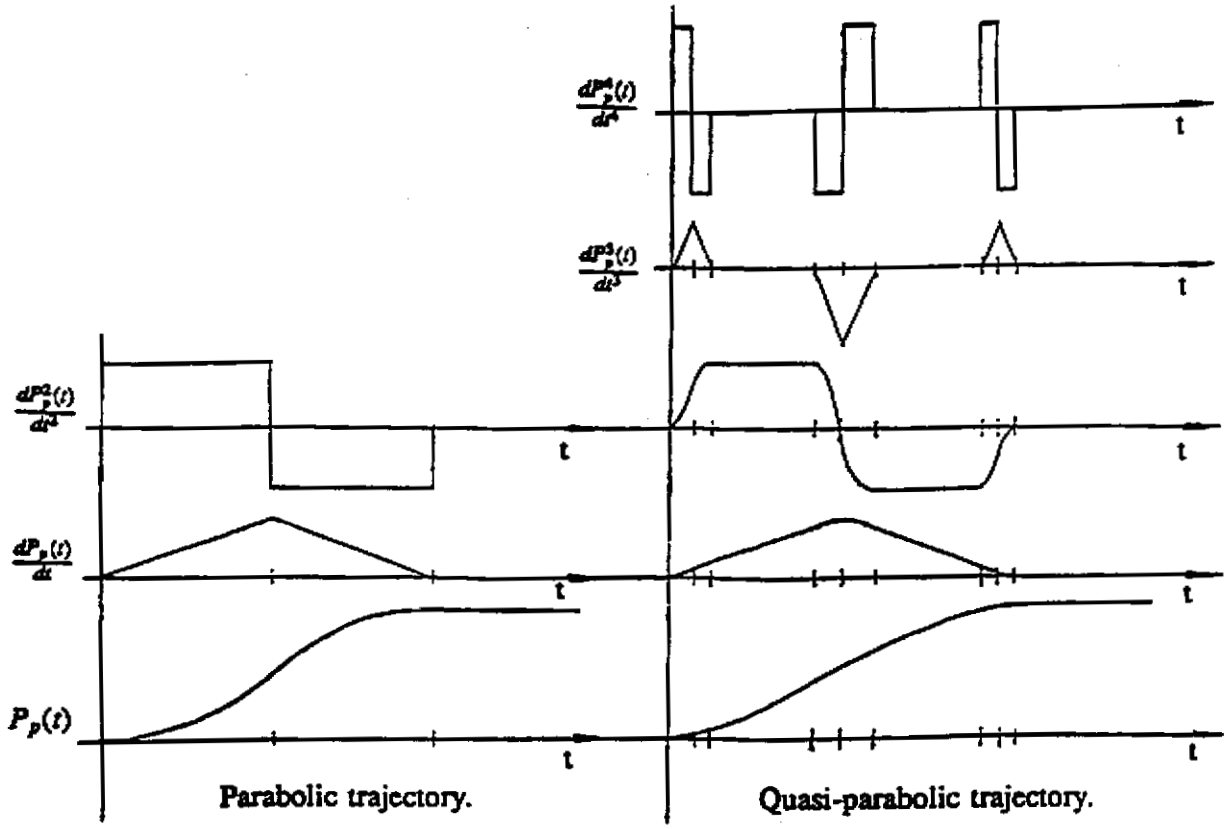


Figure 6: Nominal trajectories for the tip position ($P_p$).

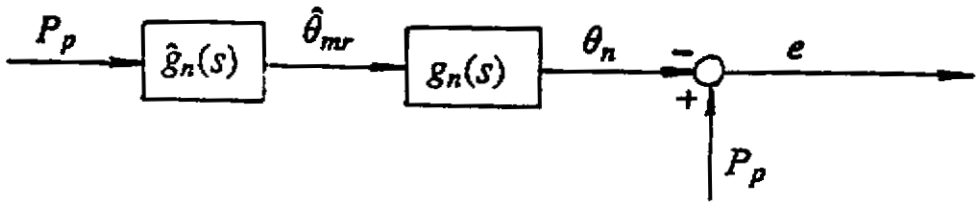


Figure 7: Feedforward control.

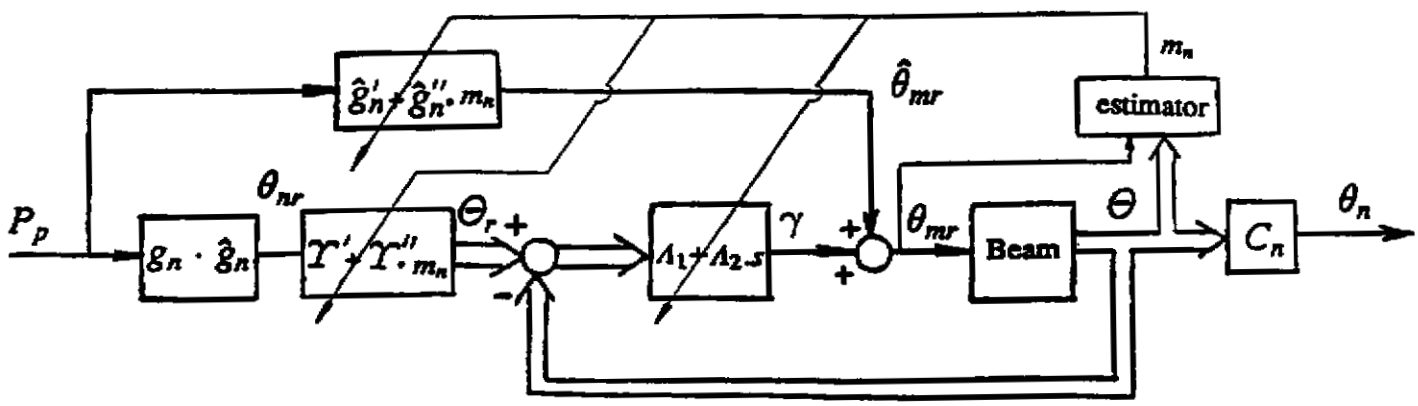


Figure 8: Adaptive general tip position control scheme.

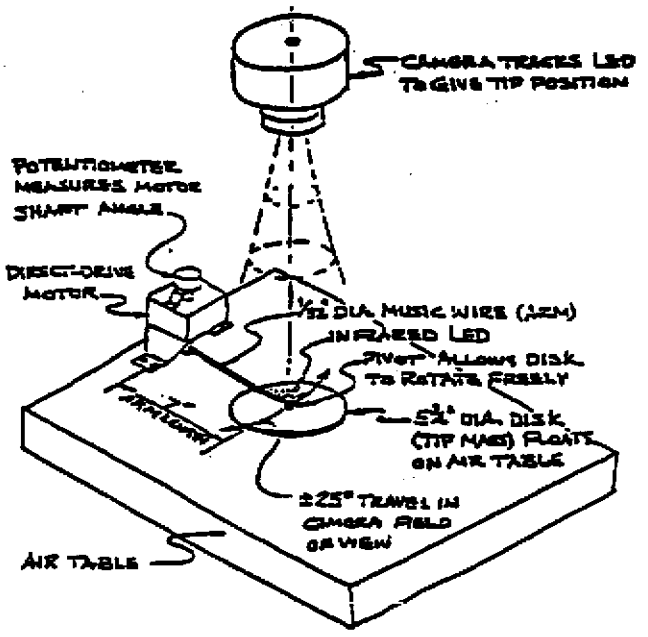


Figure 9: Experimental setup.

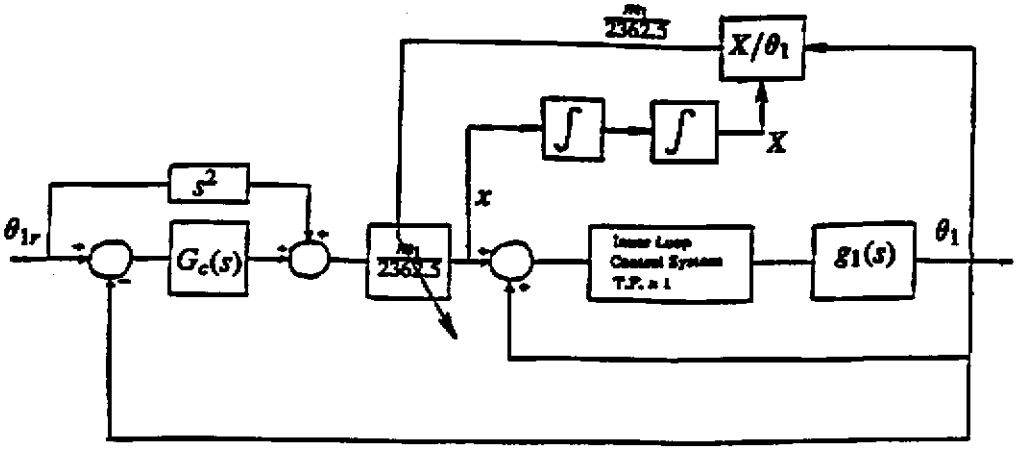


Figure 10: Adaptive scheme for the single-mass arm.

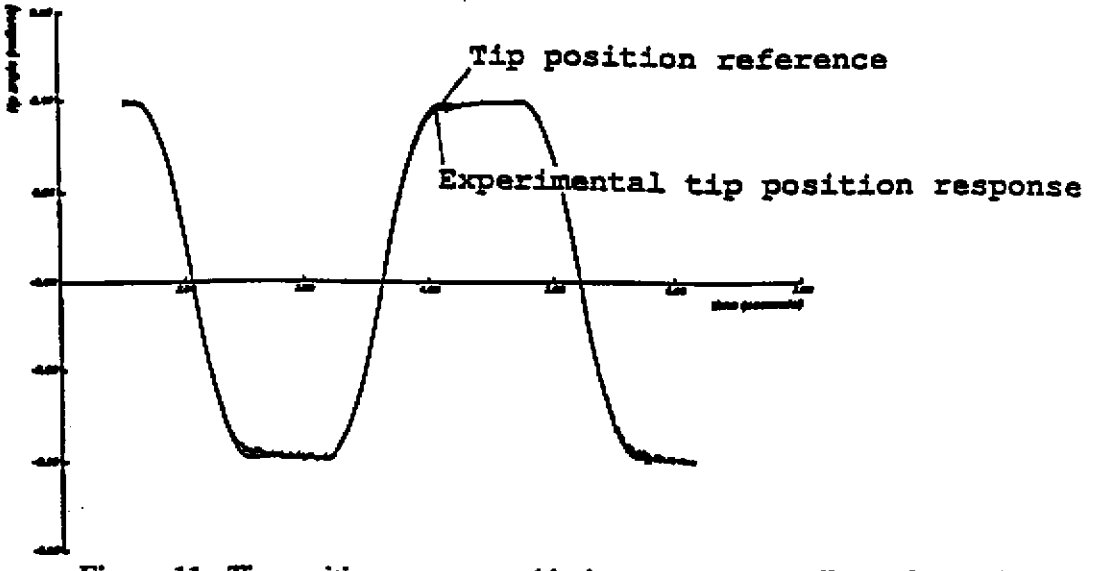


Figure 11: Tip position response with the nominal controller and a payload of 54 *gms*. (single-mass arm).

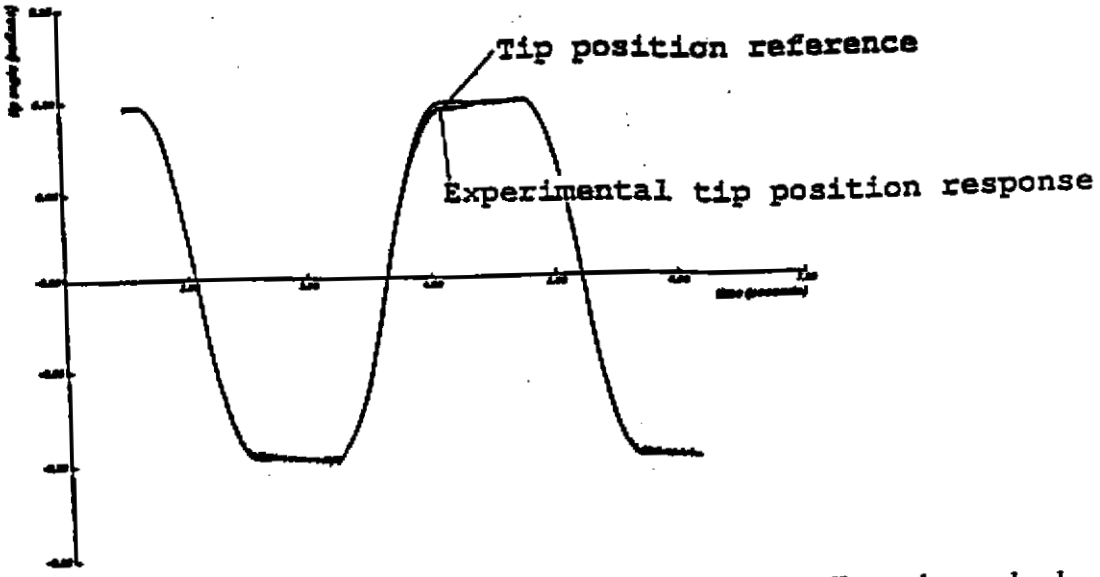


Figure 12: Tip position response with the adaptive controller and a payload of 54 *gms*. (single-mass arm).

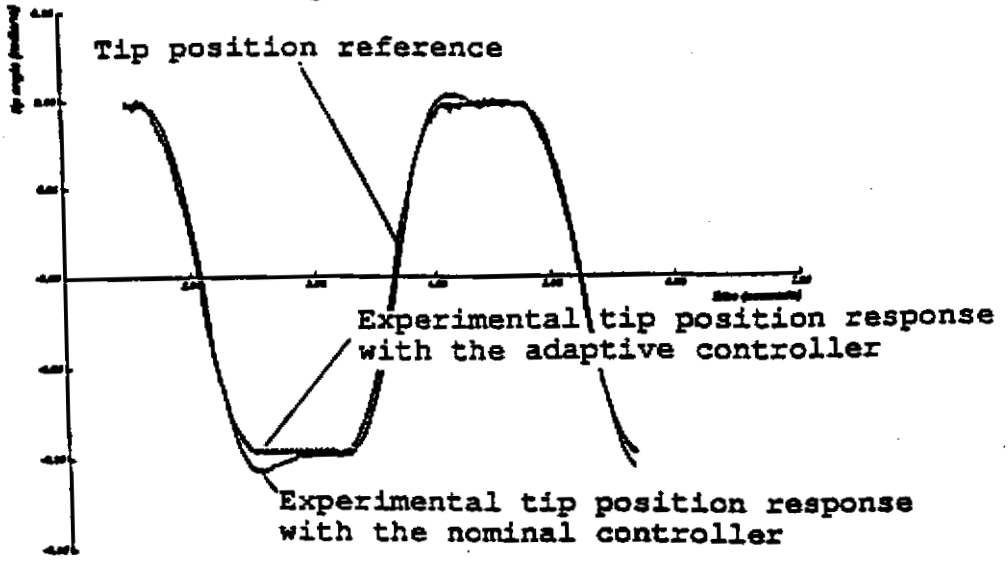


Figure 13: Tip position response of nominal and adaptive controllers with a payload of 142 *gms*. (single-mass arm).

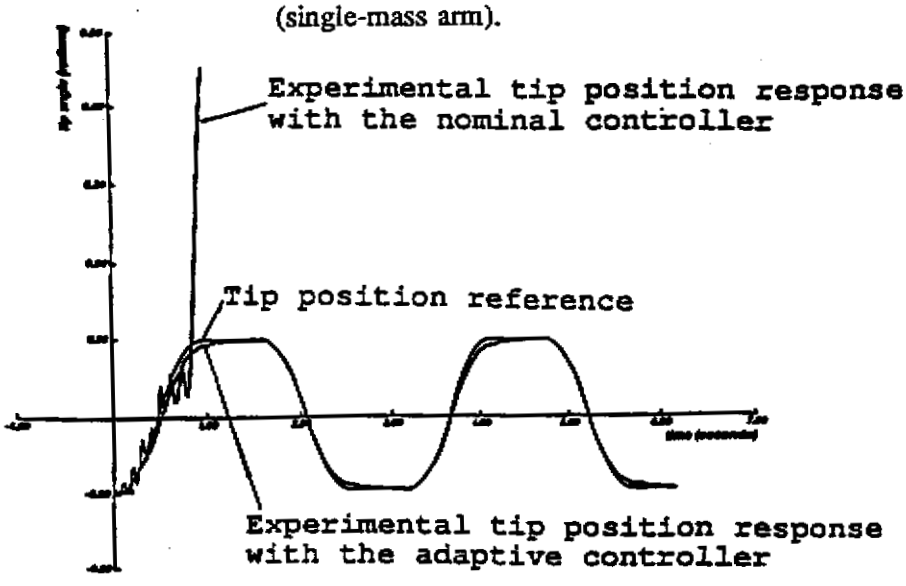


Figure 14: Tip position response of nominal and adaptive controllers with a payload of 15.73 *gms*. (single-mass arm).

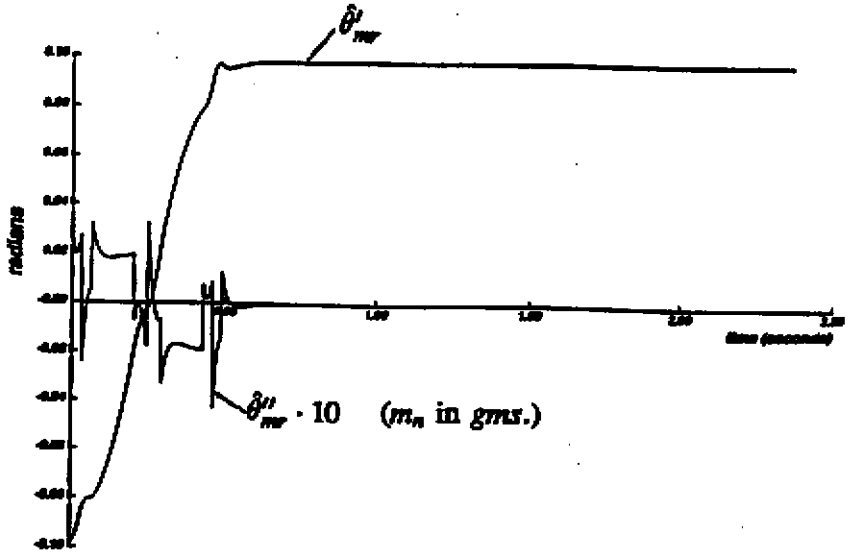


Figure 15: The two components of the feedforward signal (two-mass arm).

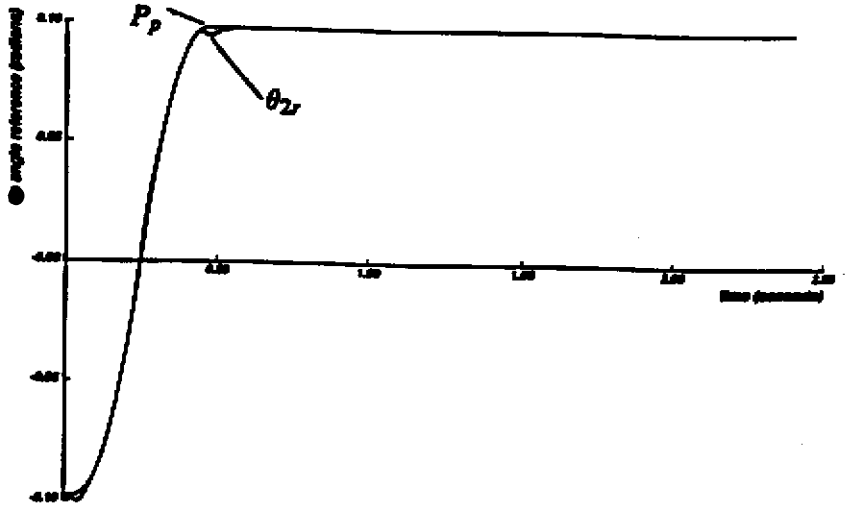


Figure 16: Nominal trajectory $P_p$ and optimum realizable reference trajectory $\theta_{2r}$ (two-mass arm).

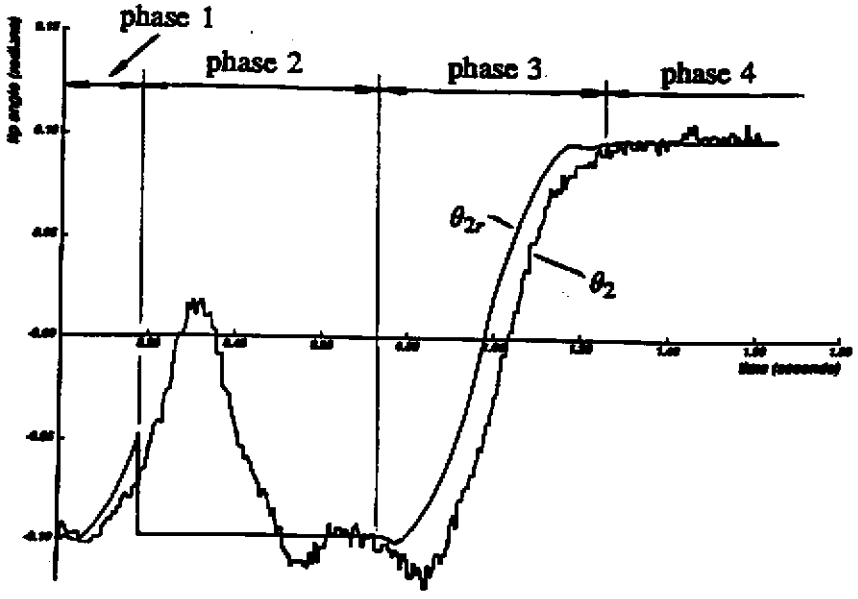


Figure 17: Tip position response of adaptive controller with a payload of 54 $gms$. (two-mass arm).

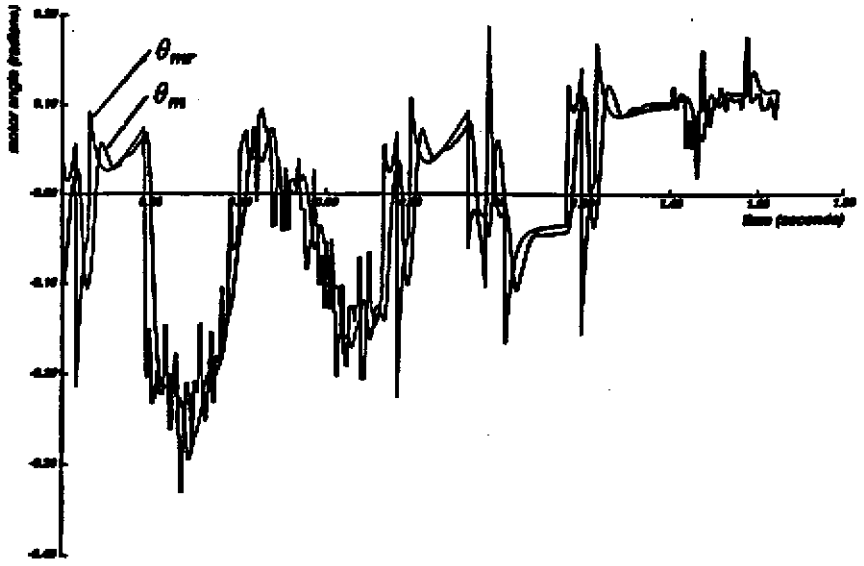


Figure 18: Motor position reference and actual motor position with a payload of 54 *gms*. (two-mass arm).

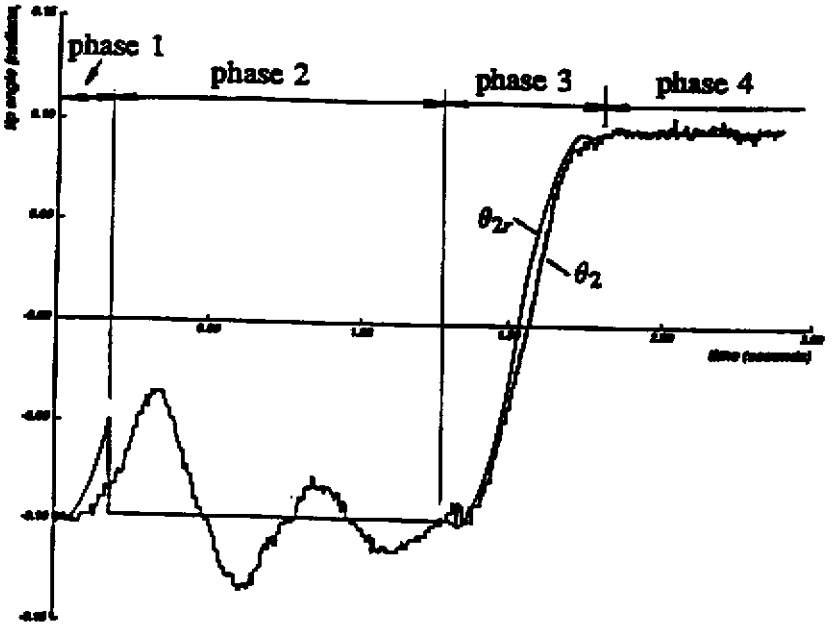


Figure 19: Tip position response of adaptive controller with a payload of 133 *gms*. (two-mass arm).

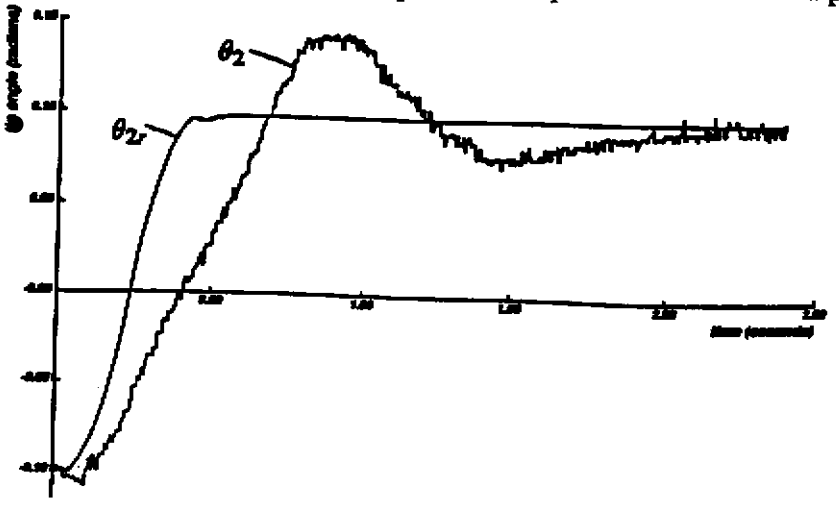


Figure 20: Tip response with a payload of 133 *gms*., and the nominal controller is used (two-mass arm).

# References


[1] Cannon, R.H. and Schmitz, E.
Precise Control of Flexible Manipulators.
*Robotics Research*, 1985.

[2] De Maria and Siciliano B.
A Multilayer Approach to Control of a Flexible Arm.
*Proceedings 1987 IEEE International Conference on Robotics and Automation.*
Raleigh (USA), April 1987.

[3] Matsuno, F., Fukushima, S. et al.
Feedback Control of a Flexible Manipulator with a Parallel Drive Mechanism.
*International Journal of Robotics Research.* Vol. 6, No. 4, Winter 1987.

[4] Ower, J. C. and Van de Vegte, J.
Classical Control Design for a Flexible Manipulator: Modeling and Control System Design.
*IEEE Journal of Robotics and Automation.* Vol. RA-3, No. 5, October 1987.

[5] Pfeiffer F. and Gebler B.
A Multistage-Approach to the Dynamics and Control of Elastic Robots.
*Proceedings 1988 IEEE International Conference on Robotics and Automation*
Philadelphia (USA), April 1988.

[6] Kotnick, T., Yurkovich, S. and Ozguner U.
Acceleration Feedback for Control of a Flexible Manipulator Arm.
*Journal of Robotic Systems.* Vol. 5, n-3, June 1988.

[7] Siciliano, B., Yuan, B.S. and Book, W.J.
Model Reference Adaptive Control of a One Link Flexible Arm.
*25th IEEE Conference on Decision and Control.* Athens, December 1986.

[8] Yuh J.
Application of Discrete-Time Model Reference Adaptive Control to a Flexible Single-Link Robot.
*Journal of Robotic Systems.* Vol. 4, n-5, 1987.

[9] Harahima, F. and Ueshiba, T.
Adaptive Control of Flexible Arm using the End-Point Position Sensing.
*Proceedings Japan-Usa Symposium of Flexible Automation*, Osaka (Japan), July 1986.

[10] Rovner, D.M. and Cannon, R.H.
Experiments Towards on-line Identification and Control of a Very Flexible One-Link Manipulator.
*International Journal of Robotics Research*, Vol. 6, No. 4, Winter 1987.

[11] Feliu, V., Rattan, K.S and Brown H.B.
A New Approach to Control Single-Link Flexible Arms. Part I: Modelling and Identification in the Presence of Joint Friction.
*CMU-RI-TR-89-8. Technical Report, Robotics Institute, Carnegie Mellon University.*

March 1989.

[12] Feliu, V., Rattan, K.S. and Brown H.B.
Modelling and Control of Single-Link Flexible Arms with Lumped Masses.
*Submitted for publication.*

[13] Rattan K.S., Feliu V. and Brown H.B.
A Robust Control Scheme for a Single-Link Flexible Manipulator with Friction in the Joints.
*Proceedings 2nd Annual USAF/NASA Workshop on Automation and Robotics*, Dayton (USA), June 1988.

[14] Truckenbrodt, A.
Dynamics and Control Methods for Moving Flexible Structures and Their Application to Industrial Robots.
*Proc. of the 5th World Congress on Theory of Machines and Mechanisms.* Montreal. 1979.

[15] Low, K. H.
A Systematic Formulation of Dynamic Equations for Robots Manipulators with Elastic Links.
*Journal of Robotic Systems.* Vol. 4(3), 1987.

[16] Feliu V., Rattan K.S. and Brown H.B.
Model Identification of a Single-Link Flexible Manipulator in the Presence of Friction.
*Proceedings of 19th ISA Annual Modelling and Simulation Conference*, Pittsburgh, May 1988.

[17] Gupta, S.C., and Hasdorff, L.
*Fundamentals of Automatic Control.* John Wiley & Sons, inc. 1970.

[18] Lee, E.B., and Markus, L.
*Foundations of Optimal Control Theory.* Krieger Publishing Co.. Florida 1986.

[19] Feliu, V., Rattan K.S. and Brown H.B.
Adaptive Control of a Single-Link Flexible Manipulator in the Presence of Joint Friction and Load Changes.
*1989 IEEE International Conference on Robotics and Automation*, Scotsdale (USA), May 1989.

[20] VanLandingham H.F.
*Introduction to Digital Control Systems.* MacMillan Publishing Company. 1985.